Neutron diffraction studies of nuclear and magnetic structures in the $S=1/2$ square Heisenberg antiferromagnets $(d_6\text{-}5CAP)_2CuX_4$ (X=Br and Cl)

F. C. Coomer, V. Bondah-Jagalu, K. J. Grant, and A. Harrison*
Department of Chemistry, The University of Edinburgh, The King's Buildings, West Mains Road, Edinburgh EH9 3JJ, United Kingdom

G. J. McIntyre
Institut Laue-Langevin, 6 Rue Jules Horowitz, Boîte Postale 156, F-38042 Grenoble Cedex 9, France

H. M. Rønnow
Laboratory for Quantum Magnetism, École Polytechnique Fédérale de Lausanne (EPFL), 1015 Lausanne, Switzerland and Laboratory for Neutron Scattering, ETH-Zürich and Paul Scherrer Institute, 5232 Villigen, Switzerland

R. Feyerherm, T. Wand, and M. Meißner
BENSC, Hahn Meitner Institut, Glienicker Straße 100, D-14109 Berlin, Germany

D. Visser
Department of Physics, Warwick University, Gibbet Hill Road, Coventry CV4 7AL, United Kingdom and The ISIS Facility, Rutherford Appleton Laboratory, Chilton, Didcot, Oxon OX11 0QR, United Kingdom

D. F. McMorrow
London Centre for Nanotechnology and Department of Physics and Astronomy, University College London, London WC1E 6BT, United Kingdon and The ISIS Facility, Rutherford Appleton Laboratory, Chilton, Didcot, Oxon OX11 0QR, United Kingdom

(Received 6 October 2005; revised manuscript received 17 October 2006; published 23 March 2007)

We report the neutron scattering studies of the nuclear and magnetic structures of deuterated samples of the model two-dimensional $S=1/2$ Heisenberg antiferromagnets on a square lattice, $(d_6\text{-}5CAP)_2CuCl_4$ and $(d_6\text{-}5CAP)_2CuBr_4$ (where 5CAP is 2-amino-5-chloropyridinium). Interest in these materials stems from the fact that they have relatively weak exchange between the magnetic ions, and it is therefore possible to perturb their magnetic structures and excitations significantly in experimentally accessible magnetic fields, and thereby access new quantum disordered states. We succeeded in growing fully deuterated single crystals and determined the nuclear and magnetic structures of the bromide at 10 and 1.8 K, respectively, confirming the four-sublattice spin structure expected for systems, where both inter- and intraplane exchange interactions are antiferromagnetic. The determination of the full crystal structure of the bromide highlights the possibility that interlayer exchange may also propagate via hydrogen bonds to and through the 5CAP molecule. We also determined the critical exponents for the sublattice magnetization of the bromide and mapped out the H-T phase diagram of the chloride up to 5 T.

DOI: 10.1103/PhysRevB.75.094424 PACS number(s): 75.40.Cx, 75.50.Ee, 61.12.−q

I. INTRODUCTION

One of the key areas of activity in fundamental solid-state magnetism today concerns the way in which quantum fluctuations lead to nonclassical behavior. Interest in this field enjoyed a resurgence after the discovery of high-temperature superconductivity in layered cuprates, whose parent compounds provide model two-dimensional (2D) $S=1/2$ (quantum) Heisenberg antiferromagnets on a square lattice (2D QHAFSL). Early magnetic measurements[1,2] suggested that the ground state of members of this class of magnet might be nonclassical, and revived much earlier models and discussions[3] of the nature of magnetic correlations in low-moment, low-dimensional magnets. While subsequent magnetic measurements of various 2D QHAFSLs indicated that the ground state and, indeed, many aspects of the one-magnon excitations are essentially classical with small corrections for quantum fluctuations, there are still surprises,[4,5] particularly when perturbed through the application of a magnetic field[6,7] or diamagnetic dilution of the magnetic lattice.[8–10]

The application of a strong magnetic field may induce mixing of the one-magnon excitations and the two-magnon continuum, destabilizing the former.[6,7] It has been predicted that the spin waves may thus become unstable with respect to two-magnon decay at a critical field H^*; for square and cubic lattices $H^* \cong 0.76H_c$ where H_c is the critical field at which the magnetization is saturated, and is equal to $(8JS)/(g\mu_B)$ (Ref. 11) for a square antiferromagnet with the following magnetic Hamiltonian:

$$H = J\sum_{\langle i,j\rangle} S_i S_j.$$

Here, the sum is over all spins i and their nearest neighbors j, and J is the corresponding exchange constant. It is not practical to explore such effects experimentally using layered cu-

TABLE I. Magnetic properties of selected $S=1/2$ Heisenberg antiferromagnets on a square lattice, J is the nearest-neighbor in-plane exchange, and H_c is the critical field at which the magnetization is saturated. Values of J'/J were calculated using an empirical expression based on QMC calculations in conjunction with experimental values of T_N and J (Ref. 25).

Compound	Jk_B^{-1} (K)	T_N (K)	T_N/J	H_c (T)	J'/J	Reference
La_2CuO_4	≅1500	310	0.21	4500	8.1×10^{-4}	22 and 23
$Sr_2CuO_2Cl_4$	≅1450	251	0.17	4300	1.11×10^{-4}	24
$Cu(COO)_24D_2O$	71.8	16.5	0.23	220	1.9×10^{-3}	14, 16, 18, and 22
$(5CAP)_2CuBr_4$	8.5	5.20	0.61	25.3	0.26	20 and 21, this work
$(5MAP)_2CuBr_4$	6.5	3.8	0.58	19.4	0.22	21
$(5CAP)_2CuCl_4$	1.25	0.754	0.60	3.62	0.25	19, this work
$(5MAP)_2CuCl_4$	0.76	0.44	0.57	2.26	0.21	19

prates on account of the high value of J (≅1500 K), requiring fields of the order of 4500 T to bring about saturation. Copper formate tetrahydrate (CFTH) and its deuterated relative (CFTD) have smaller values of J (≅72 K), and have allowed in-depth studies of the model 2D QHAFSLs (Refs. 5 and 12–18) but they too would require impractical fields to probe behavior in the region of H^* ($H_{sat}>200$ T).

An alternative model system based on a lattice of Cu^{2+} ions connected magnetically through halide ions has been prepared and characterized[19–21] and shown to have a significantly lower energy scale for J. These materials have the chemical formula $(5CAP)_2CuX_4$ or $(5MAP)_2CuX_4$ (where X=Cl or Br) (5CAP is 2-amino-5-chloropyridinium and 5MAP is 2-amino-5-methylpyridinium). Detailed heat-capacity and magnetic-susceptibility measurements yielded the magnetic parameters summarized in Table I. J takes values in the range of 0.76–8.5 K, which corresponds to saturation fields in the range of 2.3–25 T, promising access to an unprecedented range of H/J to probe the influence of quantum fluctuations on this class of magnet.

In this paper, we report neutron scattering studies of magnetic correlations in perdeuterated single crystals of $(5CAP)_2CuX_4$ (X=Br, Cl) or $(d_6\text{-}5CAP)_2CuX_4$. A different experimental setup was used for each crystal as a consequence of both the temperature range required and the availability of suitable cryostats that are also compatible with the neutron diffractometers used. In both cases, we confirmed that long-range magnetic order sets in below the values of T_N determined by previous thermodynamic measurements, and measured the sublattice magnetization. The measurements on the bromide also gave a full crystallographic structure at 10 K and a magnetic spin structure at 1.8 K. The measurements on the chloride provided rather less detailed information on the spin structure because we were only able to access a limited region of reciprocal space, but they did allow us to map out regions of the H-T phase diagram. This study provides the necessary foundation for further work on the spin dynamics of both materials.

II. EXPERIMENT

A. Synthesis and characterization

1. Preparation of single crystals of perdeuterated $(5CAP)_2CuCl_4$ and $(5CAP)_2CuBr_4$

The ligand 5CAP is not available commercially in a perdeuterated form, so it was synthesized using a modification of an established method;[26] details of this process are given in Appendix A. The ligand was then added to solutions of appropriate copper (II) halides in D_2O, and then placed in a desiccator loaded with silica gel and the solvent pulled off over the course of several weeks at room temperature (approximately 25 °C) until crystals formed. Further details of this procedure are given in Appendix B. The crystals of the chloride were orange and readily grew to volumes of the order of 10 mm^3 in the form of lozenges with well-defined faces; crystals of the bromide were dark brown and much less regular in shape.

B. Neutron diffraction measurements

1. $(d_6\text{-}5CAP)_2CuBr_4$

Neutron diffraction data for $(d_6\text{-}5CAP)_2CuBr_4$ were measured on the four-circle diffractometer D10 at the Institut Laue-Langevin, Grenoble. The largest crystal available ($6.0\times1.4\times1.4$ mm^3) had a compact form with distinct edges and faces but no obvious indication of the orientation of crystallographic axes from the crystal habit. The sample was glued with epoxy resin to a Cd sample pin and mounted in a He-flow cryostat,[27] which allows temperatures down to 2 K to be reached with little loss of four-circle access. D10 is equipped with a small two-dimensional area detector,[28] which for this measurement allowed optimal delineation of the peak from the background. Two wavelengths were used: 2.3604(6) Å using a vertically curved pyrolytic graphite (002) monochromator for measurement of the weak magnetic reflections and 1.5318(6) Å using a vertically focussing multielement Cu (200) monochromator for measurement of the higher-Q structural reflections.

Crystal structure at 10 K. Two complete sets of unique structural reflections to $\sin(\theta)/\lambda=0.40$ Å^{-1} were scanned at 10 K with a wavelength of 2.3604 Å (1134 reflections), as well as one nearly complete set of unique reflections in the range of $0.40=\sin(\theta)/\lambda=0.61$ Å^{-1} at a wavelength of 1.5318 Å (1152 reflections). Background[29] and Lorentz corrections were applied. Absorption corrections were made by Gaussian integration using the calculated attenuation coefficients $\mu=0.0528$ and 0.0386 mm^{-1} at 2.3604 and 1.5318 Å, respectively, taking into account the exchange of the labile amine deuterium atoms discussed below, giving a transmission range of 0.851–0.952. Averaging over symmetry equivalents gave 523 and 1083 unique reflections at 2.3604 and 1.5318 Å, respectively. The reflections $(h0l)$ where l is odd, which are systematically absent in space group $C2/c$, all showed small but significant contributions of similar magnitude to the nearly constant discrepancy between the observed and calculated F^2 of allowed reflections noted in the preliminary refinements of the crystal structure. We attributed this to multiple diffraction, which we could correct by subtraction of a mildly Q-dependent contribution from all observed F^2.[30] Since the three-dimensional count distribution around each reflection was observed, the centroids of all scanned reflections could be found. Least-squares matching of the observed and calculated coordinates of the centroids of the 707 strongest reflections at 2.3604 Å gave cell parameters $a=12.9032(8)$, $b=8.7577(6)$, $c=15.8324(11)$ Å, and $\beta=94.171(6)°$.

Structure refinements were made using programs based on the Cambridge Crystallographic Subroutine Library,[31] with starting coordinates taken from the room-temperature x-ray structure.[21] In all refinements, the quantity minimized was $\Sigma w(|F_{obs}|-|F_{calc}|)^2$, using weights according to $w=[\sigma^2(F^2_{obs})]^{-1}$, where σ^2 was derived from Poisson counting statistics and the population statistics within each group of equivalent reflections where these existed. Neutron scattering lengths assumed for Cu, Br, Cl, N, C, and D were 7.718, 6.79, 9.579, 9.36, 6.648, and 6.674 fm.[32] In preliminary refinements, the occupation factors of all D sites were varied to allow for possible exchange with H during or since the growth of the crystal. Indeed, this was indicated for the labile sites D(1), D(2a), and D(2b) attached to N atoms, and in later refinements, two occupation factors were varied, one for D(1) and a common factor for the chemically equivalent D(2a) and D(2b). The refined occupation factors (0.79 and 0.78) correspond to 14% exchange with H. It was also necessary to model the thermal displacement of all deuterium sites anisotropically due to the significant libration of these atoms even at 10 K. Several isotropic extinction models within the formalism of Becker and Coppens[33] were tried. The best agreement between observed and calculated data was for a type-I model with a Lorentzian distribution of mosaic blocks. The most severe extinction correction y $(|F_{obs,corrected}|^2=y|F_{obs}|^2)$ was 0.42. There were 101 variable parameters in the final structural refinement: two scale factors, the angular mosaic width, the positional and thermal displacement parameters for all 27 atoms in the asymmetric unit, and the two site occupation factors for the labile deuterium atoms. The agreement indicators following the final refinement were $R(F)=\Sigma|\Delta|/\Sigma F_{obs}=0.039$, $wR(F)=(\Sigma w\Delta^2/\Sigma wF^2_{obs})^{1/2}=0.031$, and $\chi^2=\Sigma w\Delta^2/\Sigma(n-p)=5.95$, where $\Delta=F_{obs}-|F_{calc}|$ and n and p are the number of observations and number of parameters, respectively.

Magnetic structure at 1.8 K. A limited survey of reciprocal space at 1.8 K revealed the presence of additional reflections that did not satisfy the C-centering operator of the structural space group. The strongest were (011), (101), and $(01-1)$, which were about 0.02% the intensity of the strongest structural reflection, while $(10-1)$ and all reflections with $l=0$ were unobservable. 56 reflections with $h+k=2n+1$ to $\sin(\theta)/\lambda=0.229$ Å^{-1} were scanned at both 18 and 10 K at the wavelength of 2.3604 Å. To remove the contribution from the small half-wavelength contamination, the integrated intensity of each reflection was obtained by a Gaussian fit to the difference between the ω projections of corresponding scans at 1.8 and 10 K. Lorentz and absorption corrections were applied, as described above. No correction for multiple scattering was necessary since either the operative reflection or the cooperative reflection must also fail to satisfy the C-centering operation, and is therefore too weak to lead to a significant multiple-scattering contribution.

Magnetic critical behavior. Among the reflections that had significant intensity at 1.8 K but negligible intensity at 10 K, (101) was the strongest, and this was used to determine the dependence of the sublattice magnetization on temperature from 1.8 K to temperatures in the region of 5 K (Fig. 3).

2. $(d_6\text{-}5CAP)_2CuCl_4$

Our sample of $(d_6\text{-}5CAP)_2CuCl_4$ formed lozenge-shaped crystals such that c^* was perpendicular to the faces with the largest area. The largest crystal $(5.0\times2.5\times1.5$ mm$^3)$ was oriented to a^* and c^* in the horizontal scattering plane of the neutron diffractometer. The sample was then attached to a copper pin with epoxy resin, and the pin and glue shielded with Cd before mounting in an Oxford Instruments Kelvinox dilution fridge, and placed in the core of the VM2 split-coil, vertical-field magnet (base temperature of 30 mK and maximum field of 7 T). The diffractometer was the two-axis instrument E4 located at the BER-II reactor at HMI, and was set up with 20 in. collimation on the beam incident on the sample, 40 in. collimation in front of the detector, and a neutron wavelength of 2.426 Å (PG 002).

A survey was made of likely magnetic reflections at 30 mK; scanning positions $(h0l)$ for $h=0\rightarrow3$ and for $l=-3\rightarrow3$ (the limits of these scans being set by the wavelength and the geometry of the instrument). The strongest of those reflections that are forbidden for nuclear scattering in space group $C2/c$ [space group 15 (b1) in the International Tables of Crystallography[34]] was again the (101) [we have assumed that the space group determined at 143 K by x-ray measurements is still appropriate for these low temperatures,[19] and the selection rule for this space group is h or $l=2n$ for $(h0l)$ reflections]. This was then studied as a function of tempera-

ture to determine T_N and the evolution of the sublattice magnetization. Subsequently, the temperature-field phase diagram was mapped out up to 5 T, first by observing the variation of T_N with H from neutron diffraction intensities and second by measuring the heat capacity using an Oxford Instruments MagLabHC microcalorimeter. With a ^{3}He sorption pumped insert, calorimeter temperatures as low as 0.35 K can be achieved in a magnetic-field environment up to 8 T. The single crystalline $(5CAP)_2CuCl_4$ sample (m =2.65 mg) was attached onto the sapphire chip calorimeter with a small amount of Wakefield grease (m=200 μg). The total heat capacity data were obtained by the constant heater power relaxation method where the subsequent temperature profile $\Delta T(t)$ was analyzed in terms of a 2-exponential function.[35] The heat capacity of the sample C_p was then obtained by subtracting the contributions of the sapphire chip and grease, which constituted $<5\%$ of the total.

III. RESULTS

A. $(d_6\text{-}5CAP)_2CuBr_4$

1. Crystal structure at 10 K

The geometry and atom numbering of the asymmetric unit of $(d_6\text{-}5CAP)_2CuBr_4$ produced by the structure refinement are shown in Fig. 1. Final atomic positional and equivalent isotropic displacement parameters are given in Table II and the anisotropic displacement parameters for the deuterium sites in Table III. Selected interatomic distances and interbond angles are listed in Table IV.

Our structure at 10 K is essentially the same as that determined at −130 °C by x rays,[21] although the deuterium coordinates are found to have considerably better precision in our neutron experiment. It is important for subsequent studies of the magnetic properties to know that there are no qualitative changes in the crystal structure down to low temperatures. The large distortion of the $CuBr_4^{2-}$ anion from ideally tetrahedral is observed again at 10 K, although it is not obvious from the stereochemistry why the angular distortion should be so severe. The organic cation is planar to within 0.17 Å, and all bond distances and angles within the cation lie near the average values observed for the same bonds in other compounds,[36] indicative of little intermolecular interaction. For the structurally similar 2-amino-5-methylpyridinium copper tetrabromate and tetrachlorate, it was surmised[37] that the crystal-field stabilization energy dominates the electrostatic interaction in the presence of strong hydrogen bonding to give a copper tetrahalide geometry closer to square planar than to tetrahedral. A lesser influence might be the repulsion between Br and Cl on the pyridinium ring to maintain the acceptable contact of 4.25(2) Å.

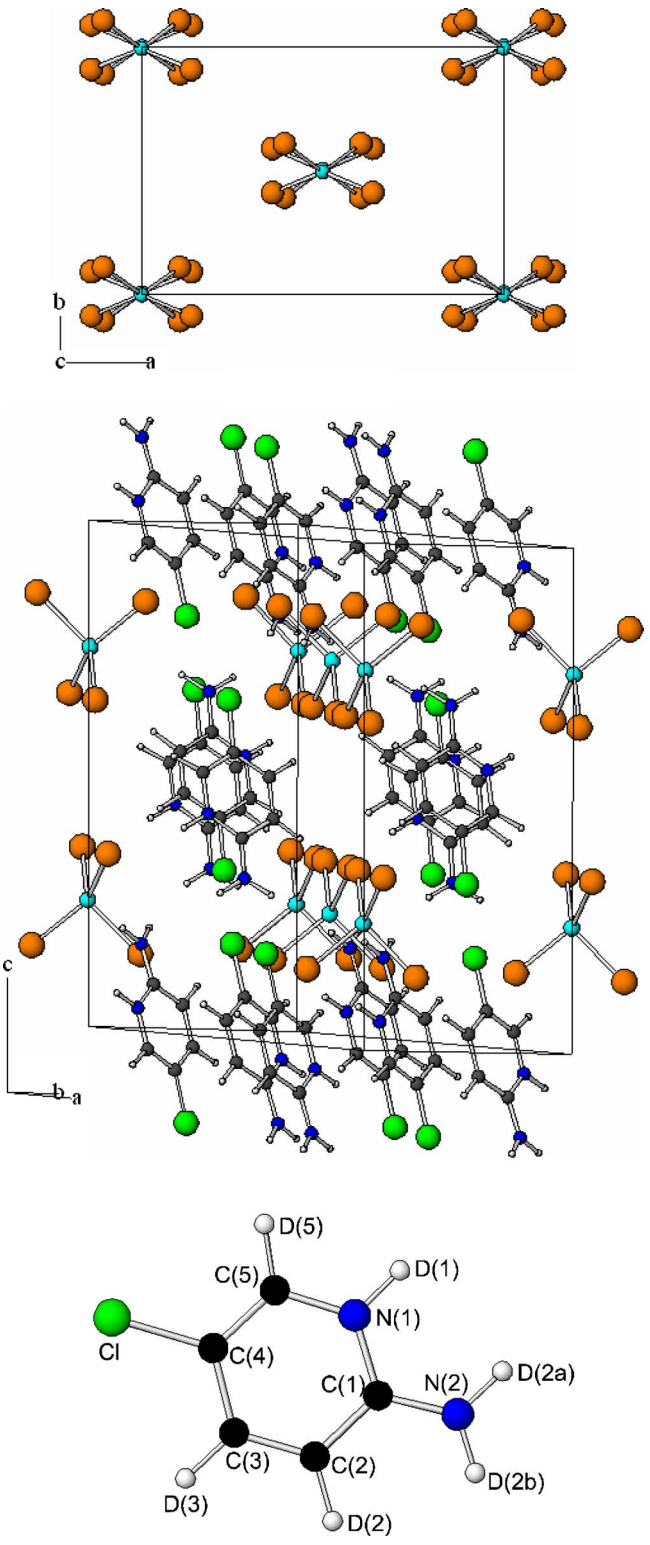

FIG. 1. (Color online) Crystal and magnetic structures of the bromide viewed (a) parallel and (b) perpendicular to the c axis. (c) shows the numbering scheme for atoms in the 5CAP molecule as used in Tables II–IV.

B. Magnetic structure at 1.8 K and sublattice magnetization

There are four Cu sites in the C centered unit cell, related by the C centering and the center of inversion. The C centering is clearly not satisfied by the magnetic structure, but it is reasonable to assume first that this might correspond simply to a reversal in the directions of the moments on the sites related by the C centering. The presence of an inversion center means that all magnetic reflections with l=0 are forbidden. That (10−1) is much weaker than (101) suggests that

TABLE II. Fractional atomic coordinates, atomic occupation factor (g), and equivalent isotropic displacement parameters (Å^2) for $(5CAP)_2CuBr_4$ at 10 K. The occupation factor is used to treat exchange of H for D at the more labile sites. The form of the displacement factor was $\exp(-2\pi^2\Sigma_i\Sigma_j U_{ij}\mathbf{h}_i\mathbf{h}_j a_i^* a_j^*)$; $U_{eq}=[U_{11}+U_{22}+U_{33})]/3$.

	x	y	z	g	U_{eq}
Cu	0	0.0050(2)	0.25		0.0009(4)
Br(1)	0.1384(1)	0.0898(2)	0.3464(1)		0.0022(4)
Br(2)	−0.1055(1)	−0.1085(2)	0.3509(1)		0.0020(4)
Cl	0.0760(1)	0.4096(1)	0.1712(1)		0.0048(3)
N(1)	0.1271(1)	0.2423(1)	−0.0530(1)		0.0033(3)
N(2)	0.1867(1)	0.3381(2)	−0.1770(1)		0.0056(3)
C(1)	0.1602(1)	0.3611(2)	−0.0983(1)		0.0024(4)
C(2)	0.1636(1)	0.5075(2)	−0.0589(1)		0.0025(4)
C(3)	0.1383(1)	0.5221(2)	0.0229(1)		0.0033(4)
C(4)	0.1061(1)	0.3931(2)	0.0679(1)		0.0030(4)
C(5)	0.0996(1)	0.2541(2)	0.0281(1)		0.0035(4)
D(1)	0.1220(2)	0.1359(2)	−0.0812(1)	0.788(8)	
D(2)	0.1862(2)	0.6050(2)	−0.0956(1)		
D(3)	0.1401(2)	0.6329(2)	0.0534(1)		
D(5)	0.0745(2)	0.1501(2)	0.0576(1)		
D(2a)	0.1771(2)	0.2367(3)	−0.2067(1)	0.777(6)	
D(2b)	0.2213(2)	0.4217(3)	−0.2078(1)	0.777(6)	

the Cu moment lies nearly along $[10-1]$. Refinement against a model with the same magnitude of moment on all four Cu sites and reversal of the directions on sites related by the C centering gave an acceptable fit with agreement indicators $R(F)=16.6$, $wR(F)=13.3$, and $\chi^2=3.86$ (cf. Table V), and a Cu moment of $0.45(1)\mu_B$ inclined 47(4)° to the c axis near $[10-1]$ within the ac plane, as illustrated in Fig. 2. Given the complex crystal structure, a number of anisotropy sources are possible, and it is difficult to argue which dominates the inclination angle.

The intensity of the strongest magnetic reflection $I(101)$ was determined as a function of temperature and field by fitting to a Gaussian curve, and all parameters were allowed to vary freely. This resulted in a stable fit with relatively little correlation between fitting parameters even close to T_N. Figure 3(a) depicts the variation of the height of the Gaussian with temperature. There was no attempt in the final fitting process to correct for scattering from critical fluctuations in the region of T_N.[38,39] The temperature dependence of $I(101)$ was analyzed by least-squares fits to the standard expression[38] for the critical exponent β for the sublattice magnetization: $I(101)=A\varepsilon^{2\beta}$, where $\varepsilon=(T_N-T)/T_N$. Optimized values from this procedure were $T_N=5.18(1)$ K and $\beta=0.23(4)$ for data taken over the temperature range of 4.95–5.17 K ($\varepsilon=0.048-0.0057$) [Fig. 3(b)]. The obtained T_N is supported by the occurrence of a cusp at this temperature in the derivative of the integrated intensity[40] [Fig. 3(c)]. This value of β is similar to that reported for other 2D QHAFSLs: CFTD (Ref. 14) displays a value of 0.23(1), crossing over to a value of 0.32(2) close to T_N ($\varepsilon<0.06$). $Sr_2CuO_2Cl_2$ (Ref. 24) yields $\beta=0.22(1)$ while for La_2CuO_4 the value of 0.28 (Ref. 41) has been reported. Since the ideal 2D Heisenberg system cannot order at finite temperature, the three-dimensional (3D) order observed in real materials is inevitably due to interlayer coupling. Therefore, the 3D critical exponents (0.326, 0.345, and 0.367 for the Ising, XY, and Heisenberg cases, respectively) can be expected sufficiently close to T_N. If the interlayer coupling is assisted by easy-

TABLE III. Anisotropic thermal displacement parameters (Å^2) for the deuterium sites in $(5CAP)_2CuBr_4$ at 10 K.

	$U11$	$U22$	$U33$	$U23$	$U12$	$U13$
D(1)	0.0166(15)	0.0051(13)	0.0123(13)	−0.0035(9)	−0.0005(10)	−0.0023(10)
D(2)	0.0228(11)	0.0103(9)	0.0147(9)	0.0023(8)	0.0014(8)	−0.0035(9)
D(3)	0.0212(11)	0.0082(9)	0.0165(9)	−0.0047(8)	0.0000(9)	−0.0011(9)
D(5)	0.0233(11)	0.0101(9)	0.0144(10)	0.0029(8)	0.0028(9)	−0.0053(9)
D(2a)	0.0229(16)	0.0096(13)	0.0156(13)	−0.0073(10)	0.0046(11)	−0.0042(11)
D(2b)	0.0222(15)	0.0134(13)	0.0105(11)	0.0033(10)	0.0053(10)	−0.0047(11)

TABLE IV. Selected interatomic distances (Å) and angles (deg) for $(5CAP)_2CuBr_4$ at 10 K. Standard deviations are given in parentheses. Footnotes on the atom symbols denote positions equivalent to those given in Table II.

		$CuBr_4$	
Cu-Br(1)	2.382(2)	Br(1)-Cu-Br(1)[a]	143.7(1)
Cu-Br(2)	2.390(2)	Br(1)-Cu-Br(2)	98.0(1)
		Br(2)-Cu-Br(1)[a]	97.9(1)
		Br(2)-Cu-Br(2)[a]	130.8(2)
		5-chloro-2-aminopyridinium	
Cl-C(4)	1.714(2)		
N(1)-C(1)	1.351(2)		
C(1)-C(2)	1.425(2)		
C(2)-C(3)	1.364(2)		
C(3)-C(4)	1.415(2)		
C(4)-C(5)	1.371(2)		
C(5)-N(1)	1.360(2)		
N(1)-D(1)	1.033(3)		
C(1)-N(2)	1.331(2)		
N(2)-D(2a)	1.007(3)		
N(2)-D(2b)	1.002(3)		
C(2)-D(2)	1.084(3)		
C(3)-D(3)	1.084(3)		
C(5)-D(5)	1.084(3)		
		Hydrogen bonds	
D(5)…Br(2)[a]	2.702(3)	C(5)-D(5)…Br(2)[a]	153.9(9)
C(5)…Br(2)[a]	3.707(3)		
D(1)…Br(1)[b]	2.302(3)	N(1)-D(1)…Br(1)[b]	170(2)
N(1)…Br(1)[b]	3.324(2)		
D(2)…Br(2)[c]	2.876(3)	C(2)-D(2)…Br(2)[c]	117.4(4)
C(2)…Br(2)[c]	3.509(2)		
D(2)…Br(1)[d]	2.879(3)	C(2)-D(2)…Br(1)[d]	147.4(7)
C(2)…Br(1)[a]	3.842(2)		
D(3)…Br(2)[a]	2.779(3)	C(3)-D(3)…Br(2)[a]	167(2)
C(3)…Br(1)[a]	3.474(2)		
D(2a)…Br(2)[e]	2.650(3)	N(2)-D(2a)…Br(2)[e]	142.9(7)
N(2)…Br(2)[e]	3.506(2)		
D(2b)…Br(2)[c]	2.868(3)	N(2)-D(2b)…Br(2)[c]	128.6(6)
N(2)…Br(2)[c]	3.580(2)		

[a] $-x, y, 1/2+z$.
[b] $x, -y, -1/2-z$.
[c] $1/2+x, 1/2-y, -1/2-z$.
[d] $-x, 1+y, 1/2+z$.
[e] $-x, -y, -z$.

plane anisotropy, one might at lower temperature anticipate a crossover to the Bramwell-Holdsworth value of approximately 0.23 for β.[24,42–44] Indeed, such a crossover is observed in CFTD, while the more 2D $Sr_2CuO_2Cl_2$ perhaps only reaches 3D exponents closer to T_N than hitherto experimentally accessed. Dedicated critical scattering experiments, on $(d_6\text{-}5CAP)_2CuBr_4$ and the other model materials, would be warranted for a better understanding of the order and extent of crossover regions, as well as the alternatively proposed $\beta=0.25$ due to the proximity of a tricritical point in La_2CuO_4.[45]

TABLE V. Observed and calculated structure factors for $(5CAP)_2CuBr_4$ at 1.8 K. The total 56 measured reflections were reduced to 34 inequivalent reflections.

h	k	l	F_{obs}	F_{calc}
1	0	0	0.000(15)	0
−2	1	0	0.000(15)	0.012253
0	1	0	0.000(15)	0.015754
−1	2	0	0.000(15)	0.028258
−1	0	1	0.000(15)	0.012754
1	0	1	0.551(17)	0.47163
3	0	1	0.243(31)	0.36710
−2	1	1	0.251(20)	0.28808
0	1	1	0.558(26)	0.45162
2	1	1	0.366(16)	0.41962
−3	2	1	0.329(23)	0.30633
−1	2	1	0.417(24)	0.40061
1	2	1	0.443(33)	0.43262
3	2	1	0.351(26)	0.36410
−2	3	1	0.384(41)	0.34234
0	3	1	0.370(23)	0.38711
2	3	1	0.312(73)	0.36535
−1	0	2	0.000(15)	0
1	0	2	0.000(15)	0
0	1	2	0.000(15)	0.013754
−3	0	3	0.000(15)	0.011003
−1	0	3	0.179(29)	0.22006
1	0	3	0.314(27)	0.43137
3	0	3	0.464(26)	0.40236
−2	1	3	0.211(22)	0.20056
0	1	3	0.344(19)	0.37810
2	1	3	0.436(19)	0.42287
−3	2	3	0.199(21)	0.23581
−1	2	3	0.335(41)	0.33634
1	2	3	0.453(42)	0.40061
3	2	3	0.332(37)	0.36860
−2	3	3	0.319(32)	0.29583
0	3	3	0.420(26)	0.35160
2	3	3	0.284(33)	0.35110

There has been some debate on the overall form of $M(T)$ for quantum 2D systems, with the proposal that a $T \ln T$ law is expected as $M(T)$ tends to the $T=0$ saturation value, $M(0)$,[46–48] and a mean-field dependence, with $\beta=0.5$ closer to T_N.[49] Being limited to $T>1.75\ \mathrm{K} \sim T_N/3$, we cannot address the low-temperature limit of $M(T)$. Attempts were also made to observe scattering from short-range correlations above T_N by scanning in a direction perpendicular to c^* through $(0-10.2475)$ but the scattering was too weak to merit further study with this sample.

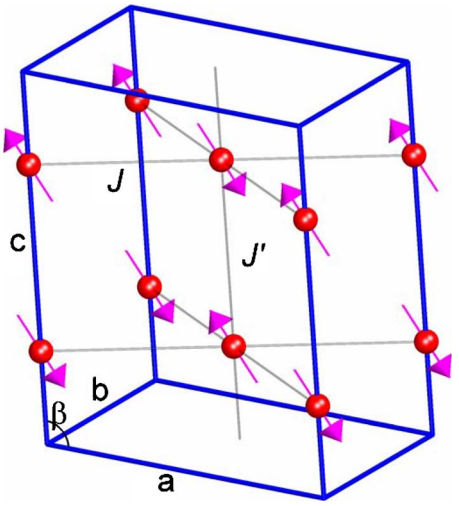

FIG. 2. (Color online) Magnetic structure depicting the copper sites of the unit cell, with the moment direction indicated by the arrows. The nearest-neighbor intralayer coupling J and interlayer coupling J' are indicated by the gray lines.

C. $(d_6\text{-}5CAP)_2CuCl_4$

Significant scattering intensity was observed in the a^*c^* plane of (5CAP) copper (II) chloride at (101), (10−1), (301), and (30−1) despite being in contravention of the reflection condition for nuclear scattering in space group 15 (b1); weaker reflections of this type were also observed at (103), (10−3), and (303). The observed reflections and their relative intensities were consistent with the structure derived for $(d_6\text{-}5CAP)_2CuBr_4$, as depicted in Fig. 2, but the number of reflections were insufficient for a refinement of the magnetic moment and its inclination angle. The intensity of all of these reflections was reduced to negligible levels by the application of a 5.0 T field perpendicular to the scattering plane, thereby proving their magnetic origin.

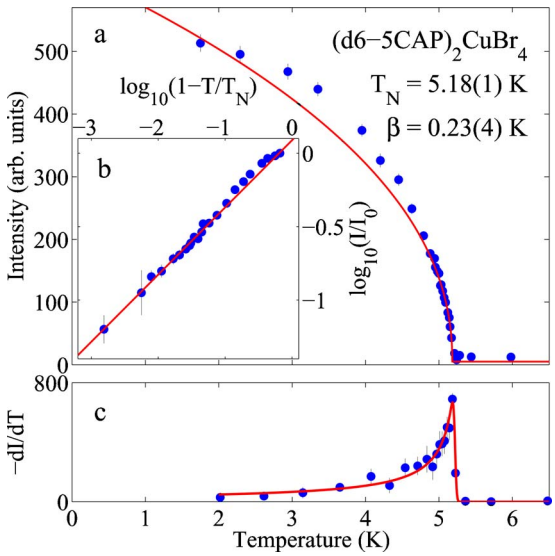

FIG. 3. (Color online) (a) Dependence of $I(101)$ on temperature for (5CAP) copper (II) bromide in zero applied field. Data have been corrected for background scattering. The line is a fit to the standard power-law expression $I(T)=A\varepsilon^{2\beta}$, where $\varepsilon=[1-(T/T_N)]$, yielding $T_N=5.18(1)$ K and $\beta=0.23(4)$. (b) The same data in a log-log plot. (c) The derivative of the total integrated intensity, $-dI/dT$, as a function of temperature showing a cusp at T_N.

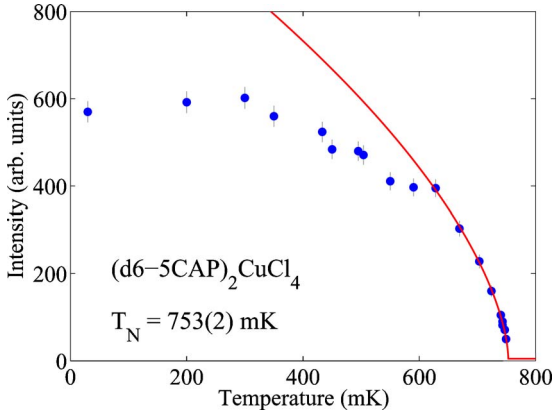

FIG. 4. (Color online) Dependence of $I(101)$ on temperature for (5CAP) copper (II) chloride in zero applied field. Data have been corrected for background. We deduce the transition temperature $T_N=754(5)$ mK.

The treatment of data from the measurement of $I(101)$ as a function of temperature and magnetic field was the same as for the bromide. Figure 4 depicts the variation of $I(101)$ with temperature yielding $T_N=754(2)$ mK.

The dependence of $I(101)$ on magnetic field applied perpendicular to the a^*c^* plane was measured at several fixed temperatures as a function of the field perpendicular to the a^*c^* plane (Fig. 5). At the base temperature of 30 mK, the intensity disappeared at a field $H_c=3.62(3)$ T, above which the magnetic moments should be fully polarized with the field. As the temperature was raised toward T_N, H_c decreased toward zero. The corresponding phase diagram is depicted in Fig. 6. Further data were taken at temperatures between 670 and 754 mK, but the weakness of the scattering made it very

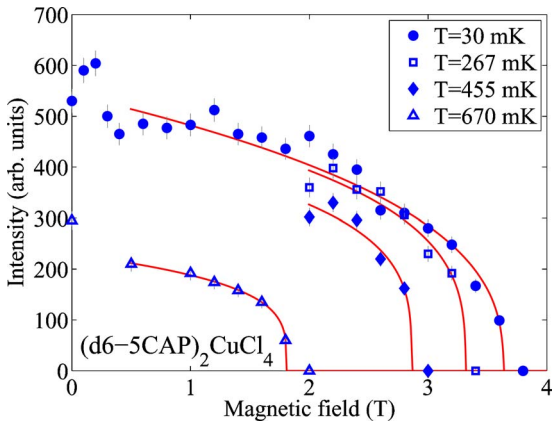

FIG. 5. (Color online) Variation of $I(101)$ for (5CAP) copper (II) chloride with applied field at selected temperatures denoted by the symbols: 30 mK (closed circles), 267 mK (open circles), 455 mK (closed triangles), and 670 mK (open triangles). The black lines are guides to the eye. Data were taken in 0.2 T steps up to and beyond the point where no scattering intensity was observed above the background.

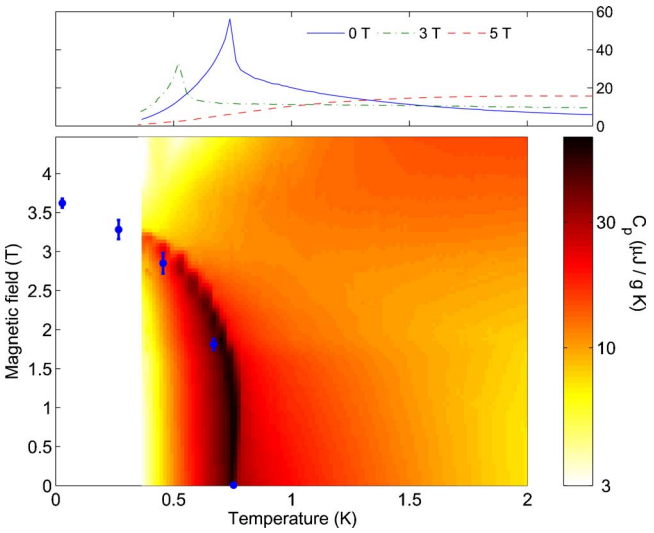

FIG. 6. (Color online) *H-T* phase diagram for (5CAP) copper (II) chloride determined by neutron scattering and specific heat measurements. The solid points are the critical fields obtained by tracking the neutron scattering intensity $I(101)$ at fixed temperatures as a function of magnetic field applied along the *b* axis (Fig. 4). The top panel shows the heat capacity, $C_p(T,H)$, as a function of temperature for three constant magnetic fields ($H=0$, 3, and 5 T) applied perpendicular to the *b* axis. $C_p(T,H)$ was measured in a temperature range $T=0.35-12$ K for a total of 11 different fields, from which the color map of C_p vs temperature and field was constructed. To allow direct comparison with the neutron scattering data, the magnetic-field scale for the C_p data has been scaled by the *g* factors (Ref. 21) $g_{ac}/g_b=2.06/2.22$. The peak in C_p traces the phase transition to the antiferromagnetic phase in good accord with the neutron scattering data.

difficult to determine T_N with sufficient accuracy to contribute usefully to this phase diagram for reasonable counting times. Instead, to obtain more detailed information on the phase boundary, we also show in Fig. 6 the heat capacity C_p as a function of temperature and magnetic field. The antiferromagnetic transition is identified as a sharp peak in $C_p(T)$, which is in good agreement with the neutron scattering data. An anomaly in the neutron scattering intensity was observed as a function of field at 35 mK and 0.2–0.3 T, and could point to a spin-flop transition as suggested by ac susceptibility measurements on the 5MAP analog.[19]

IV. DISCUSSION

It has been noted before that both the materials studied in this work have significant interplane magnetic exchange.[21] Although the structure has a layered form with the 5CAP ligands separating planes of CuX_4^{2-} tetrahedra (X=Cl,Br), the pathways for intra- and interplane exchanges, respectively J and J', are not particularly dissimilar, all passing through Cu-*X*-*X*-Cu bridges. Our measurements reveal a ratio of in-plane to out-of-plane Br-Br distances of 1.17 at 10 K (with individual values of 4.23 and 4.84 Å, respectively), while Hammar *et al.* found this ratio to be 1.138 for X=Cl (with individual values of in-plane and out-of-plane Cl-Cl separations of 4.34 and 4.94 Å, respectively).[19] There are relatively few materials in which superexchange through Cu-*X*-*X*-Cu (X=Cl,Br), bridges exists and has been characterized.[50,51] These exceptions include $ACuCl_3$ materials (A=Rb,Cs) with a distorted hexagonal perovskite structure in which there are chains of distorted, face-sharing $CuCl_6^{4-}$ octahedra lying along the *c* axis. Analysis of susceptibility and ESR data for the cesium salt[52–54] yielded values of intra- and interchain exchanges $J/k_B=28$ K and $J'/k_B=-5$ K, respectively, while the Cl-Cl distance in the interchain Cu-Cl-Cl-Cu pathway was 3.596 Å. The bromide analogs have quite different structures,[55,56] and no such comparisons may be made, although there are other $ACuBr_3$ chain materials in which Br-Br contacts may provide exchange pathways—for example, $(C_6H_{11}NH_3)CuBr_3$ [cyclohexyl ammonium tribromocuprate(II) (CHAB)].[57–59] Here, the strength of the interchain exchange interaction is of the order of 0.1–0.01 K and may contain contributions from dipole-dipole coupling (the in-chain exchange is ferromagnetic), as well as small contributions from superexchange, which might propagate either through Cu-Br-Br-Cu pathways or through hydrogen bonds from Br to both protons of the $-NH_2$ groups. In the former pathway, the Br-Br separation is approximately 5.05 Å, while the Br-D separation in a deuterated form of the latter is 2.33–2.44 Å.[58] Similar behavior is found for the corresponding chloride $(C_6H_{11}NH_3)CuBr_3$ (CHAC), with interchain exchange interaction about half that in CHAB, Cl-Cl separation in a potential Cu-Cl-Cl-Cu pathway of 4.94 Å, and Cl-D bond lengths for a potential Cu-Cl-D-N-D-Cl-Cu pathway of 2.41–2.42 Å.[60]

It is often stated that superexchange strength decreases rapidly with increasing separation of the orbitals that convey the spin information, but there have been relatively few attempts to quantify the relationship, and these are limited to specific types of exchange pathways, none of which are directly applicable to the present case. Where a relationship has been established, it has commonly been found to take the form $J\sim r^{-n}$, where the exponent n typically ranges from 9 to 12, and is most commonly 10.[60–63] It should be noted that most of this work applies to 180° M-O-M or M-F-M bridges. If we apply this relationship with $n=10$ and take r to refer just to the *X*-*X* separation, we find ratios of J'/J of 0.27 and 0.21 for X=Cl and Br, respectively. Perhaps fortuitously this corresponds closely to the calculated values for this ratio using an empirical relation based on quantum Monte Carlo (QMC) calculations for anisotropic cubic lattices in which the exchange (J') is weaker along one cell axis than the other two (J).[25] For values of $0.001<J'/J<1$, it was proposed that for $S=1/2$, the following relationship holds:

$$T_N = 2.30J/[2.43 - \ln(J'/J)].$$

The values of J'/J, calculated either with this expression or, for smaller values of J'/J, an extended variant, are given in Table I for selected 2D QHAFSLs. Note that within the *ab* layers, there is just one short Br-Br separation between $CuBr_4^{2-}$ units, but two such between layers,[21] so the ratio J'/J in the implementation of the QMC method should be replaced by $2J'/J$, where each exchange constant refers to a

single exchange pathway. It should also be noted that the disposition of magnetic atoms and exchange pathways between layers is quite different in these materials compared to La_2CuO_4 and related, layered cuprates, as well as in CFTD and CFTH; in these other materials, copper sites in one layer are displaced by $(\frac{1}{2},\frac{1}{2})$ relative to those in adjacent layers, and the different interlayer exchange interactions sum up to zero. Both these factors conspire to make J'/J larger for both $(5CAP)_2CuX_4$ compounds.

Other exchange pathways may also be significant in these materials. For the bromide, the shortest separation between Br and D atoms coordinated to nitrogen is 2.303 Å. In addition, exchange may propagate via the 5CAP molecules: there are several different D-Br separations (Table IV), the smallest being 2.302 Å [D(5)-Br(2)], and several in the range of 2.65–2.8 Å [D(2a)-Br(2), D(5)-Br(2), and D(3)-Br(2)]; similar pathways have been shown to be responsible for exchange interactions between Cu^{2+} ions of the order of $1-2\ \mathrm{cm}^{-1}$ $(J/k_B \cong 1.2-2.9\ \mathrm{K})$.[64] Of course, the materials studied here differ from those in previous studies in their being predominantly deuterated. However, this is expected to lead to relatively small changes in exchange interactions, with a modest reduction anticipated when H is substituted by D.[65,66] Figure 7 shows these hydrogen bonds for $(d_6\text{-}5CAP)_2CuBr_4$, together with the shortest Br-Br separations. This points to methods of improving the magnetic anisotropy through the use of the longer, less-conjugated organic species—though, of course, 5CAP is likely to play a role in the formation of this particular type of structure, possibly through relatively weak covalent interactions involving its π system, and replacement by quite a different organic species could lead to quite different structures.

V. CONCLUSIONS

We have used single-crystal neutron diffraction to study the nuclear and magnetic structures of deuterated samples of the model two-dimensional $S=1/2$ square Heisenberg antiferromagnets $(d_6\text{-}5CAP)_2CuCl_4$ and $(d_6\text{-}5CAP)_2CuBr_4$. Our magnetic measurements confirm previous susceptibility studies that demonstrated antiferromagnetic coupling within and between the magnetic layers, with a modest degree of anisotropy: application of a recently derived empirical relationship between J, J', and T_N indicates J'/J to be of the order of 0.1 (i.e., the ratio of the total inter- to intraplane exchange couplings is 0.2 taking into account the relative number of inter- and intraplane exchange pathways). Consideration of the crystal structure of the bromide indicates that the 5CAP molecules may also play a role in intra- and interlayer coupling, being hydrogen bonded to Br as well as providing a conjugated system for delocalization of spin polarization. Similar effects almost certainly come into play in the chloride analogs.

In summary, the temperature dependence of the sublattice magnetization for both materials is compatible with those expected for quasi-2D antiferromagnets, and the general features of the H-T phase diagram of the chloride up to 5 T as well as the static spin structure of the bromide all appear quite conventional. Our results thereby provide the necessary foundation for further work to explore nonclassical behavior in applied magnetic fields where H/J is large.[7] To our knowledge, $(d_6\text{-}5CAP)_2CuCl_4$ is the only candidate model material in which the saturation field is accessible to inelastic neutron scattering $(H_s < 15\ \mathrm{T})$, and for which large crystals have successfully been grown.

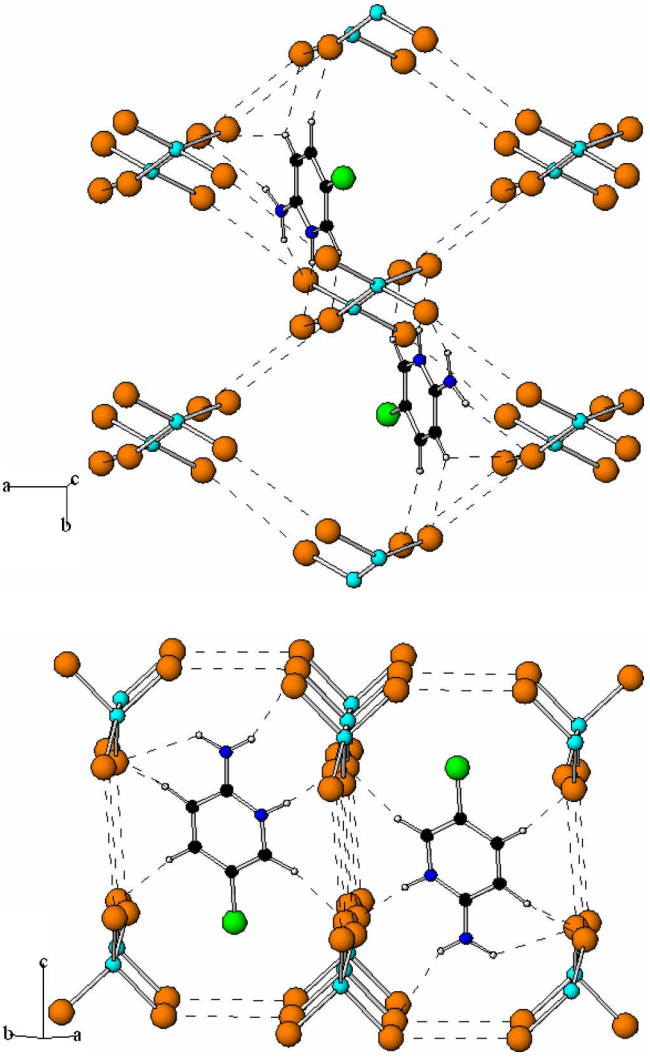

FIG. 7. (Color online) Crystal structure of the bromide viewed (a) nearly parallel and (b) perpendicular to the c axis along $\boldsymbol{a}+\boldsymbol{b}$, with closest Br–Br separations and shortest Br–D separations indicated by the dashed lines.

Although the deduced values of J'/J are not as good as for previously studied model systems, the effect of J' is small away from the 3D critical region. Furthermore, it is believed that the predictions for behavior in high magnetic fields are robust toward significant 3D interactions.[7] In fact, the existence of intermediate J'/J materials such as $(d_6\text{-}5CAP)_2CuX_4$ may become advantageous. There have recently been both numerical and analytical scaling predictions for quasi-2D Heisenberg antiferromagnets.[25,67] To test these predictions, a series of different materials spanning a range in J'/J must be investigated.

Nevertheless, there is still a need to produce better examples of model 2D QHAFSLs, and, in particular, to de-

crease the ratio J'/J while keeping J/k_B below 5 K (corresponding to a saturation field of 15 T—the maximum currently achievable for neutron scattering). One way ahead could be to add bulky functional groups to the 5CAP molecules, but the probability that a similar structure will form is low, so until there is a quantum leap in the power of computational prediction of the structure of molecular materials, we rely on intuition and the synthesis of many new compounds with $S=1/2$ centers to provide such models.[68]

ACKNOWLEDGMENTS

We are grateful to the UK EPSRC for financial support, and also to the Institut Laue-Langevin, Grenoble and the Hahn-Meitner Institute for access to beam time and technical support.

APPENDIX A: SYNTHESIS OF PER-*D*-2-AMINO-5-CHLOROPYRIDINE

Per-*d*-2-aminopyridine (4.95 g, 49.5 mmol) was dissolved in 72% D_2SO_4 (Aldrich) (25 ml) and treated with a slow infusion of Cl_2 gas [generated from solid $KMnO_4$ (Aldrich, 3.4 g) and concentrated HCl (25 ml), equating to 1 mol equivalence of chlorine, which was precondensed into a small tube cooled by dry ice and subsequently allowed to boil off very slowly]. This reaction mixture was allowed to reflux at approximately −30 °C for approximately 8 h before it was allowed to warm to room temperature (≅293 K). The reaction mixture was then carefully treated with NaOD solution [approximately 50% in D_2O, preprepared from D_2O and sodium metal under nitrogen (care)] until the *p*H of the resulting mixture was approximately 12. Following dilution with D_2O (Aldrich, approximately 30 ml), the resulting Na_2SO_4 was filtered off and sucked as dry as possible on a frit. The solid product was washed further with D_2O (approximately 300 ml), until nearly all had dissolved. NaCl (s) was added to the latter D_2O washings, until no more salt would dissolve, and the saturated solution was extracted with ethyl acetate (3 × approximately 50 ml), dried over $NaSO_4$, filtered, and concentrated *in vacuo* to yield the title ligand as a white crystalline solid (1.6 g, 24%). This was shown by electron-impact mass spectrometry to have a m/z of 133.5, five mass units greater than the nondeuterated analog, with no other peaks below this that would indicate exchange of deuterons to protons.

APPENDIX B: PREPARATION OF SINGLE CRYSTALS OF PERDEUTERATED $(5CAP)_2CuCl_4$ and $(5CAP)_2CuBr_4$

To anhydrous copper (II) chloride (Aldrich, 0.69 g, 5.13 mmol, 1 eq) was added DCl (37 wt %, 1.04 ml, 10.26 mmol, 2 eq), followed by D_2O (approximately 20 ml). The resulting mixture was stirred for about 1 min before the deuterated ligand (1.37 g, 10.26 mmol, 2 eq) was added portionwise. The resulting mixture was heated gently until all of the solid which had formed dissolved completely. The green solution was then filtered into a 50 ml beaker which had been pretreated [with 10% dimethyldichlorosilane (Aldrich) in ethanol, emptied and washed with acetone and dried in the oven]. This beaker was then placed in a sealed desiccator which held freshly dried self-indicating silica gel. The desiccator was left undisturbed for at least 6 weeks during which time the solution became a deeper green before orange crystals of the title compound $(d_6\text{-}5CAP)_2CuCl_4$ were observed. (d_6-5CAP) copper (II) bromide was crystallized in an analogous manner to the chloride: to 20 ml of D_2O were added anhydrous copper (II) bromide (Aldrich, 2.23 g, 10 mmol, 1 eq), DBr (47 wt %, 2.27 ml, 20 mmol, 2 eq), and the organic ligand (2.67 g, 20 mmol, 2 eq). The crystals typically took eight weeks to grow to a size suitable for neutron diffraction (>10 mm^3).

*Author to whom correspondence should be addressed. Email address: a.harrison@ed.ac.uk

[1] E. Manousakis, Rev. Mod. Phys. **63**, 1 (1991).
[2] G. Shirane, Y. Endoh, R. J. Birgeneau, M. A. Kastner, Y. Hidaka, M. Oda, M. Suzuki, and T. Murakami, Phys. Rev. Lett. **59**, 1613 (1987).
[3] P. W. Anderson, Science **235**, 1196 (1987).
[4] Y. J. Kim, A. Aharony, R. J. Birgeneau, F. C. Chou, O. Entin-Wohlman, R. W. Erwin, M. Greven, A. B. Harris, M. A. Kastner, I. Ya. Korenblit, Y. S. Lee, and G. Shirane, Phys. Rev. Lett. **83**, 852 (1999).
[5] N. B. Christensen, H. M. Rønnow, D. F. McMorrow, A. Harrison, G. Aeppli, T. G. Perring, R. Coldea, L. P. Regnault, and M. Enderle (unpublished).
[6] K. Osano, H. Shiba, and Y. Endoh, Prog. Theor. Phys. **67**, 995 (1982).
[7] M. E. Zhitomirsky and A. L. Chernyshev, Phys. Rev. Lett. **82**, 4536 (1999).
[8] A. L. Chernyshev, Y. C. Chen, and A. H. Castro Neto, Phys. Rev. B **65**, 104407 (2002).
[9] O. P. Vajk, P. K. Mang, M. Greven, P. M. Gehring, and J. W. Lynn, Science **295**, 1691 (2002).
[10] A. W. Sandvik, Phys. Rev. B **66**, 024418 (2002).
[11] J. C. Bonner and M. E. Fisher, Phys. Rev. **135**, A640 (1964).
[12] A. Harrison, S. J. Clarke, T. E. Mason, and D. Visser, J. Magn. Magn. Mater. **104**, 557 (1992).
[13] S. J. Clarke and A. Harrison, J. Phys.: Condens. Matter **4**, 6217 (1992).
[14] S. J. Clarke, A. Harrison, T. E. Mason, G. J. McIntyre, and D. Visser, J. Phys.: Condens. Matter **4**, L71 (1992).
[15] S. J. Clarke and A. Harrison, J. Magn. Magn. Mater. **140**, 1627 (1995).
[16] H. M. Ronnow, D. F. McMorrow, and A. Harrison, Phys. Rev. Lett. **82**, 3152 (1999).
[17] H. M. Ronnow, D. F. McMorrow, A. Harrison, I. D. Yongson, R. Coldea, T. G. Perring, G. Aeppli, and O. Syljuasen, J. Magn. Magn. Mater. **236**, 4 (2001).
[18] H. M. Ronnow, D. F. McMorrow, R. Coldea, A. Harrison, I. D.

Youngson, T. G. Perring, G. Aeppli, O. Syljuasen, K. Lefmann, and C. Rischel, Phys. Rev. Lett. **87**, 037202 (2001).
[19] P. R. Hammar, D. C. Dender, D. H. Reich, A. S. Albrecht, and C. P. Landee, J. Appl. Phys. **81**, 4615 (1997).
[20] T. Matsumoto, Y. Miyazaki, A. S. Albrecht, C. P. Landee, M. M. Turnbull, and M. Sorai, J. Phys. Chem. B **104**, 9993 (2000).
[21] F. M. Woodward, A. S. Albrecht, C. M. Wynn, C. P. Landee, and M. M. Turnbull, Phys. Rev. B **65**, 144412 (2002).
[22] Y. Endoh, K. Yamada, R. J. Birgeneau, D. R. Gabbe, H. P. Jenssen, M. A. Kastner, C. J. Peters, P. J. Picone, T. R. Thurston, J. M. Tranquada, G. Shirane, Y. Hidaka, M. Oda, Y. Enomoto, M. Suzuki, and T. Murakami, Phys. Rev. B **37**, 7443 (1988).
[23] R. Coldea, S. M. Hayden, G. Aeppli, T. G. Perring, C. D. Frost, T. E. Mason, S.-W. Cheong, and Z. Fisk, Phys. Rev. Lett. **86**, 5377 (2001).
[24] M. Greven, R. J. Birgeneau, Y. Endoh, M. A. Kastner, M. Matsuda, and G. Shirane, Z. Phys. B: Condens. Matter **96**, 465 (1995).
[25] C. Yasuda, S. Todo, K. Hukushima, F. Alet, M. Keller, M. Troyer, and H. Takayama, Phys. Rev. Lett. **94**, 217201 (2005).
[26] T. J. Kress, L. L. Moore, and S. M. Costantino, J. Org. Chem. **41**, 93 (1976).
[27] C. M. E. Zeyen, R. Chagnon, F. Disdier, and H. Morin, Rev. Phys. Appl. **19**, 789 (1984).
[28] M. S. Lehmann, W. F. Kuhs, G. J. McIntyre, C. Wilkinson, and J. R. Allibon, J. Appl. Crystallogr. **22**, 562 (1989).
[29] C. Wilkinson, H. W. Khamis, R. F. D. Stansfield, and G. J. McIntyre, J. Appl. Crystallogr. **21**, 471 (1988).
[30] J. Luzon, C. Dobe, J. Barratt, and G. J. McIntyre (personal communication).
[31] J. C. Matthewman, P. Thompson, and P. J. Brown, J. Appl. Crystallogr. **15**, 167 (1982).
[32] V. F. Sears, in *Methods of Experimental Physics*, edited by K. S. D. L. Price (Academic, Orlando, 1986), Vol. 23A, p. 521.
[33] P. J. Becker and P. Coppens, Acta Crystallogr., Sect. A: Cryst. Phys., Diffr., Theor. Gen. Crystallogr. **30**, 129 (1974).
[34] T. Hahn, in *International Tables for Crystallography* (Kluwer, Dordrecht, 1992), Vol. A.
[35] M. Meissner and P. Strehlow, J. Low Temp. Phys. **137**, 355 (2004).
[36] F. H. Allen, P. G. Watson, L. Brammer, A. G. Orpen, and R. Taylor, in *International Tables for Crystallography*, edited by A. J. C. Wilson and E. Prince (Kluwer, Dordrecht, 1999), Vol. C, p. 788.
[37] H. Place and R. D. Willett, Acta Crystallogr., Sect. C: Cryst. Struct. Commun. **43**, 1050 (1987).
[38] M. F. Collins, *Magnetic Critical Scattering* (OUP, Oxford, 1989).
[39] A. Harrison, M. F. Collins, J. Abu-Dayyeh, and C. V. Stager, Phys. Rev. B **43**, 679 (1991).
[40] A. D. Bruce, J. Phys. C **14**, 193 (1981).
[41] B. Keimer, N. Belk, R. J. Birgeneau, A. Cassanho, C. Y. Chen, M. Greven, M. A. Kastner, A. Aharony, Y. Endoh, R. W. Erwin, and G. Shirane, Phys. Rev. B **46**, 14034 (1992).
[42] S. T. Bramwell and P. C. W. Holdsworth, J. Appl. Phys. **73**, 6096 (1993).
[43] S. T. Bramwell and P. C. W. Holdsworth, J. Phys.: Condens. Matter **5**, L53 (1993).
[44] S. T. Bramwell and P. C. W. Holdsworth, Phys. Rev. B **49**, 8811 (1994).
[45] T. Thio and A. Aharony, Phys. Rev. Lett. **73**, 894 (1994).
[46] A. Singh, Z. Tesanovic, H. Tang, G. Xiao, C. L. Chien, and J. C. Walker, Phys. Rev. Lett. **64**, 2571 (1990).
[47] N. Rosov, Phys. Rev. Lett. **67**, 1938 (1991).
[48] A. Singh, Z. Tesanovic, H. Tang, G. Xiao, C. L. Chien, and J. C. Walker, Phys. Rev. Lett. **67**, 1939 (1991).
[49] P. Kopietz, Phys. Rev. Lett. **68**, 3480 (1992).
[50] M. F. Collins and O. A. Petrenko, Can. J. Phys. **75**, 605 (1997).
[51] L. J. de Jongh and A. R. Miedema, Adv. Phys. **50**, 947 (2001).
[52] Y. Tazuke, H. Tanaka, K. Iio, and K. Nagata, J. Phys. Soc. Jpn. **50**, 3919 (1981).
[53] H. Hyodo, K. Iio, and K. Nagata, J. Phys. Soc. Jpn. **50**, 1545 (1981).
[54] H. Tanaka, U. Schotte, and K. D. Schotte, J. Phys. Soc. Jpn. **61**, 1344 (1992).
[55] M. Inoue, M. Kishita, and M. Kubo, Inorg. Chem. **6**, 900 (1967).
[56] T. Li and G. D. Stucky, Inorg. Chem. **12**, 441 (1973).
[57] K. Kopinga, A. M. C. Tinus, and W. J. M. de Jonge, Phys. Rev. B **25**, 4685 (1982).
[58] G. C. de Vries, R. B. Helmholdt, E. Frikkee, K. Kopinga, W. J. M. de Jonge, and E. F. Godefroi, J. Phys. Chem. Solids **48**, 803 (1987).
[59] K. Kopinga, T. Delica, and H. Leschke, Phys. Rev. B **40**, 7239 (1989).
[60] H. A. Groenendijk, H. W. J. Blote, A. J. Van Duyneveldt, R. M. Gaura, C. P. Landee, and R. D. Willett, Physica B & C **106**, 47 (1981).
[61] D. Bloch, J. Phys. Chem. Solids **27**, 881 (1966).
[62] L. J. de Jongh and R. Block, Physica B & C **79**, 568 (1975).
[63] S. T. Bramwell, J. Phys.: Condens. Matter **2**, 7527 (1990).
[64] A. Luque, J. Sertucha, L. Lezama, T. Rojo, and P. Roman, J. Chem. Soc. Dalton Trans. **1997**, 847.
[65] M. M. Matsushita, A. Izuoka, T. Sugawara, T. Kobayashi, N. Wada, N. Takeda, and M. Ishikawa, J. Am. Chem. Soc. **119**, 4369 (1997).
[66] H. Tsujii, Z. Honda, B. Andraka, K. Katsumata, and Y. Takano, Phys. Rev. B **71**, 014426 (2005).
[67] M. B. Hastings and C. Mudry, Phys. Rev. Lett. **96**, 027215 (2006).
[68] A. Harrison, J. Phys.: Condens. Matter **16**, S553 (2004).